Supplementary file 1

doi:10.34172/bi.31358
https://bi.tbzmed.ac.ir/

Computational analysis on design and optimization of low-frequency dielectrophoretic microfluidic lab on a chip for *Staphylococcus aureus* isolation from blood

Saeed Saedy[1], Navid Alaei-sheini[1*], Shahrzad Ajabi[1], Karim Ansari-Asl[1]

[1]Faculty of Engineering, Shahid Chamran University of Ahvaz, Ahvaz, Iran

As shown in **Figure S1**, in the absence of an electric field, the particles exit through the first outlet due to the dominant effects of velocity and drag force.

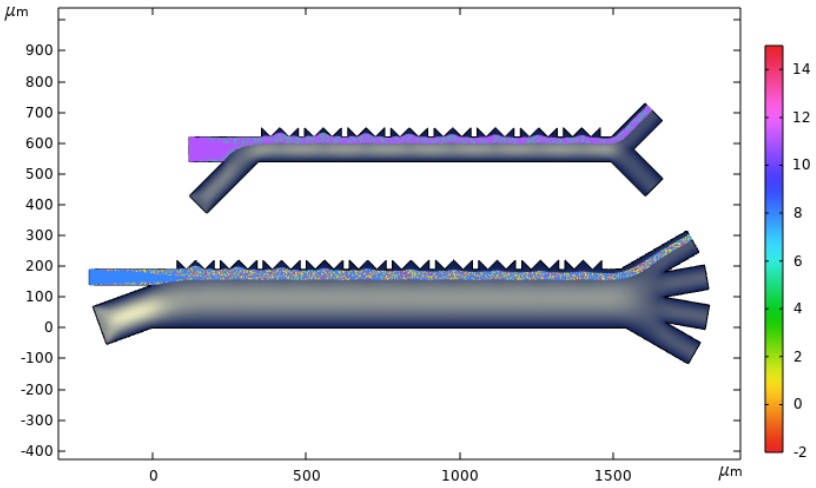

Figure S1. Particle trajectory without an electric field.

Dielectric characterization of cells via relative permittivity. **Figure.S2(A)** Permittivity values for cellular constituents of blood (WBCs, RBCs, PLTs). **Figure.S2(B)** Permittivity contrast between the antibiotic-resistant (MRSA) and antibiotic-susceptible (MSSA) strains of S. aureus.

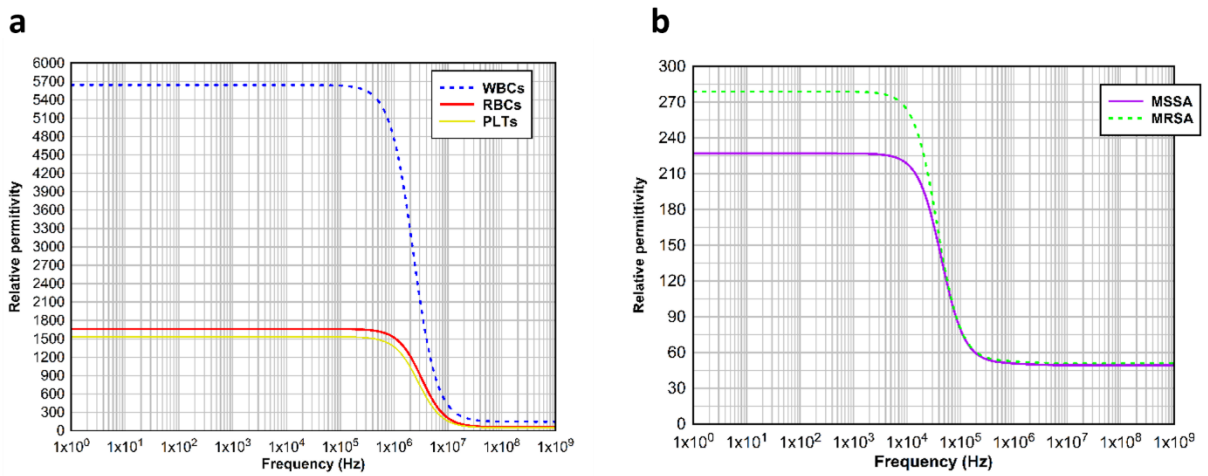

Figure.S2. Relative permittivity of (A) WBCs, RBCs, PLTs; (B) MRSA, MSSA.

Revised Channel Model Incorporating MRSA-Specific CM Factor at Low Frequencies

Although our study primarily focuses on typical Gram-positive bacteria, experimental findings from Roziani et al. [26 in manuscript] demonstrate that MRSA exhibits a positive Clausius-Mossotti factor, R[CM(f)], at frequencies below 2 MHz. Considering these experimentally observed dielectric characteristics, we have introduced a tailored channel design that incorporates this behavior. This modified design is described in detail in the supplementary file and aims to better capture the unique dielectrophoretic response of MRSA under low-frequency conditions.

In their 2023 study, Rozaini et al, demonstrated the use of DEP for the label-free characterization of antibiotic resistance in Staphylococcus aureus by monitoring changes in crossover frequency (f_{xo}). They established distinct baseline f_{xo} values for MSSA and MRSA strains at 6–8 MHz and 2–3 MHz, respectively. A key finding was a significant and opposing shift in these values upon antibiotic exposure. Furthermore, they reported an unexpected R[CM(f)] factor behavior: experimentally, MRSA exhibited a positive R[CM(f)] factor at lower frequencies, contrary to simulations which predicted a negative value. These findings are summarized in **Figure S3**.

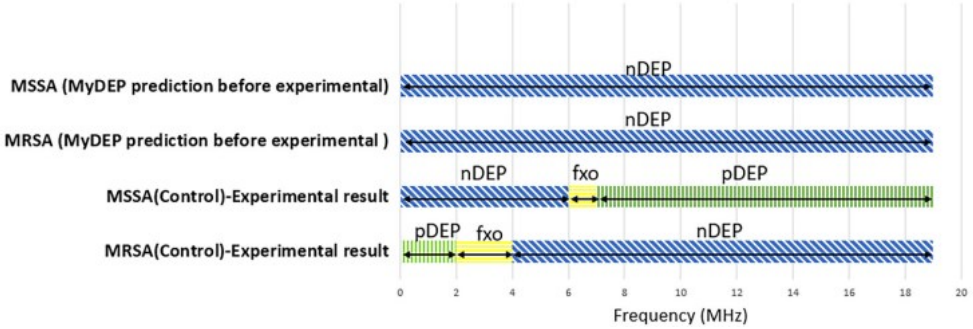

Figure S3. Experimental vs. simulated DEP response of S. aureus. Depiction of the distinct baseline f_{xo} values for MRSA and MSSA and the unexpected positive CM factor for MRSA observed experimentally.

Their study identified a CM factor plot that closely aligned with the experimental data **Figure S4**; this validated plot was consequently adopted for our supplementary simulations.

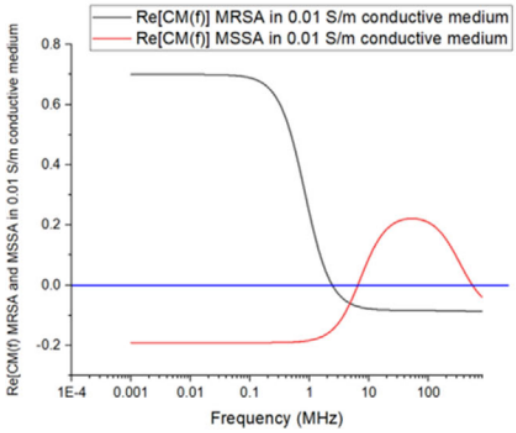

Figure S4. Validated CM factor plot from literature used for simulation.

As shown in Figure S4, at 1 kHz, MSSA exhibits nDEP (Re[CM] ≈ -0.18), while MRSA exhibits pDEP (Re[CM] ≈ 0.66). This contrast in DEP response enables separation within our microfluidic chip. The process requires an initial centrifugation to remove platelets. The first separation stage then isolates bacteria from WBCs and RBCs, utilizing a combination of DEP force and hydrodynamic flow (facilitated by a larger bacteria outlet).

To minimize the attraction of MRSA to high-gradient electric field regions, two buffer inlets were used with a flow velocity three times greater than the sample inlet (600 µm/s vs. 200 µm/s). This hydrodynamic focusing keeps MRSA farther from the electrodes. The applied voltage was also lowered to 4 V to deliberately decrease the pDEP force on MRSA. Consequently, the channel width was decreased to 100 µm to ensure a suitable DEP effect on RBCs and WBCs.

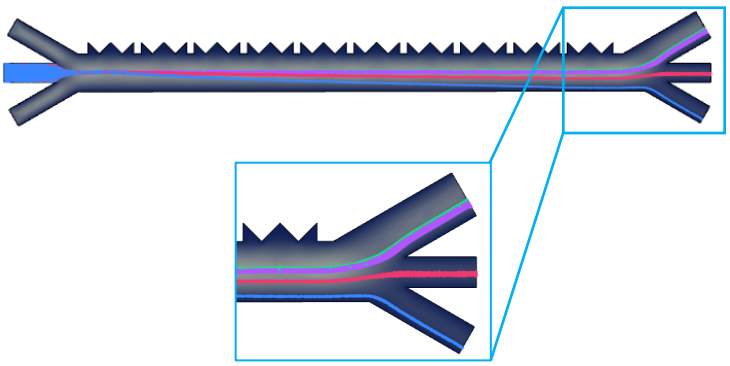

Figure S5. Overview of the first channel.

The dimensions and sizes of the first channel are shown in **Figure S6**, while those of the second channel are the same as described in the manuscript.

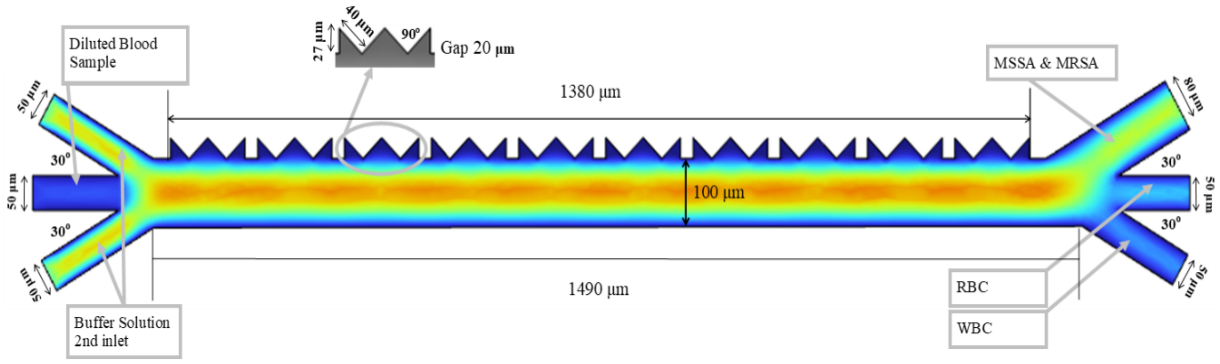

Figure S6. Dimension of the first channel.

On the other hand, in the second stage, we attempted to separate the bacterial species using two different frequency regimes. As shown in **Figure S7(A)**, a low frequency of 1 kHz was applied with a sample-to-buffer flow velocity ratio of 1000:200 µm/s and an applied voltage of 27 V. At this frequency, MRSA exhibits a positive Re[CM(f)], causing it to experience pDEP and migrate toward regions of high electric field gradient. To enhance separation, the sample inlet was offset to increase the distance between MRSA and the high-field region. However, this configuration resulted in insufficient separation efficiency and poor purity, as both bacterial populations remained largely overlapping.

In contrast, as illustrated in **Figure S7(B)**, we employed a frequency of 3 MHz, where MRSA lies within the crossover region, where Re[CM(f)] ≈ 0 resulting in negligible DEP force acting on MRSA, as supported by the data in **Figures S3-S4**. Under these conditions, MSSA exhibits a lower Re[CM(f)], leading to effective separation via nDEP. The electrode voltage was set to 35 V, and the sample-to-buffer flow velocity ratio was optimized to 400:800 µm/s. Under this configuration, clear and efficient separation of MRSA and MSSA was achieved, as evidenced by high separation purity and efficacy in **Figure S7(B)**.

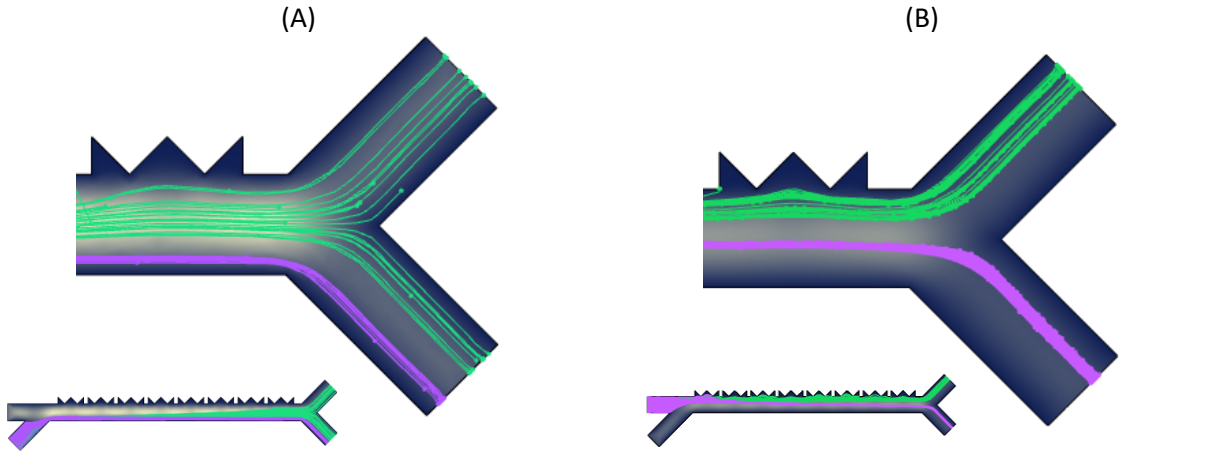

Figure S7. Particle trajectories of bacteria in the second channel. (A) MRSA under pDEP conditions and MSSA under nDEP conditions. (B) MRSA at crossover frequency and MSSA under nDEP conditions.